Versatile spectrometry in an educational environment

M. de Bock, Science and Technology of Nuclear Fusion, Applied Physics,
Eindhoven University of Technology, The Netherlands (November 2012)

Application Note

Introduction

In (university) education hands-on experiments play an ever more important role. It is no longer sufficient to just study books. The students should be able to familiarize themselves with the methods and technology used commonly in research and industry. This requires modern equipment that is applicable in a wide range of projects.

This application note focuses on the Shamrock SR-500i-B1 spectrograph in combination with the iVac DR324B-FI CCD detector (both from Andor Technology) that are used to support student projects in the Science and Technology of Nuclear Fusion group at the Eindhoven University of Technology (TU/e) in the Netherlands.

Important factors in the choice of the spectrometer system were:

- Availability to a number of projects
- Ease of use

The first point is ensured by the fact that the Shamrock SR-500i-B1 combines a small size, hence a large mobility, with large modularity in the form of a 3 grating-turret and choices between different entrance and exit slits and ports. The former allows to choose between a wide spectral range at lower spectral resolution or a smaller spectral range at high spectral resolution. The choice between an exit port with the iVac CCD or an exit slit allows to use the system either as spectrograph or as monochromator.

The SOLIS Windows spectroscopy and imaging software provides a GUI enabling control of the spectroscopic system, measurement and logging (of the system settings) without a steep learning curve.

Below 2 student projects that made use of the Shamrock/iVac spectrometer system are described to give a flavour of the use of this system in a university environment. Both student projects did overlap in time, with the test setups located in different (but adjacent) labs. The spectrometer was placed on a movable table and an SMA fibre-coupling setup was mounted to the entrance slit. This allowed to quickly move the spectrometer from one lab to the next and coupling the light of the setup in question by just attaching a fibre.

Interference filter tuning for MSE measurements

In a first project the changes in the band shape of thin film interference filters when illuminated under an angle was investigated. The angle of the incident light on an interference filter determines the central wavelength of the band pass (see Figure 3). This effect is used to select the correct part of the Motional Stark Effect (MSE) spectrum in tokamak fusion reactors.

Tokamak fusion reactors use a magnetic field B to confine a plasma at the high temperatures required for nuclear fusion reactions (15keV or ~150,000,000 °C). That magnetic field consist of a known externally applied toroidal field $B\varphi$ and a poloidal field $B\theta$ induced by the a priori unknown distribution of the current distribution in the tokamak (see Figure 1). Due to the high temperatures probes cannot be used to determine the direction of the magnetic field (and hence the distribution of the current). Therefore, techniques based on (visible) light are used, one of which is the MSE diagnostic.

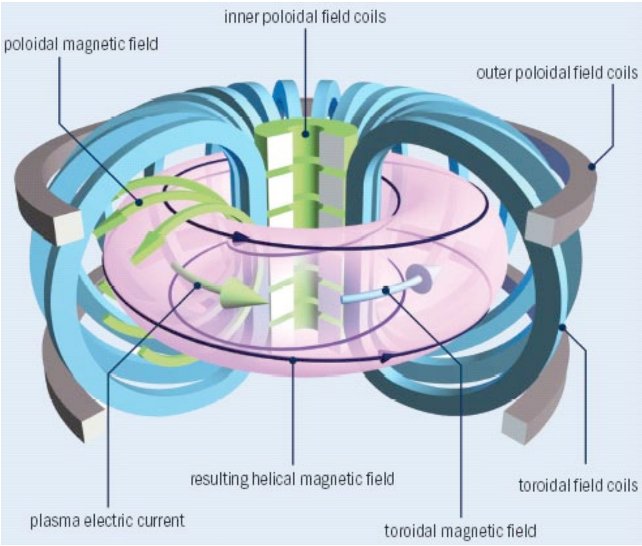

Figure 1 - Principle of a tokamak fusion reactor (www.EFDA.org).

MSE spectra are emitted by a beam of neutral particles (typically the Balmer-α emission of hydrogen) injected at a known velocity v into the plasma. The Balmer-α line emission will be Doppler shifted due to the velocity v and Stark splitted due to the Lorentz electric field $v \times B$ in the frame of reference of the moving beam particles. The polarization of the emission lines is either parallel (π-lines) or perpendicular (σ-lines) to $v \times B$ and, because v is known, contains the vital information on the direction of the confining magnetic field B (see Figure 2). To

Versatile spectrometry in an educational environment

M. de Bock, Science and Technology of Nuclear Fusion, Applied Physics,
Eindhoven University of Technology, The Netherlands (November 2012)

determine this polarization either the π- or σ-lines are filtered out and there polarization angle determined.

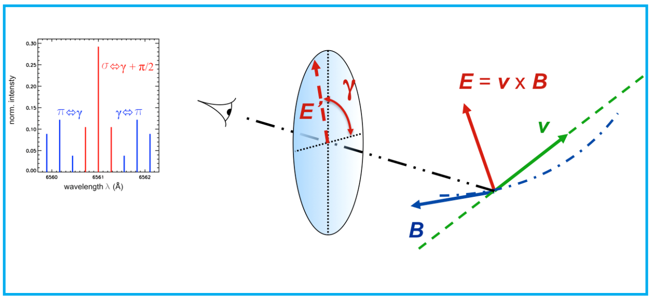

Figure 2 - Principle of MSE. A beam of hydrogen particles is injected with known velocity *v*. The Balmer-α emission is Stark splitted due to the Lorentz electric field *vxB*. The Stark lines are polarized either parallel (π) or perpendicular (σ) to the Lorentz field and hence contain information on the magnetic field *B*.

However, the central wavelength of interference filters has a certain manufacturing tolerance and the beam velocity v and the magnetic field strength B can vary a little from experiment to experiment. This is the reason why tilting of interference filters is used to control their central wavelength.

Apart from shifting the central wavelength, tilting the interference filter also changes the band shape. This is due to the fact that the incident light is never a perfectly parallel bundle, but has a certain divergence (see Figure 3). The research questions of this student project were:

- Can we find a model that predicts the changes in band shape and matches to measurements of the band shape for tilted filters?
- How does the changed band shape influence the MSE measurement compared to an unchanged band shape?

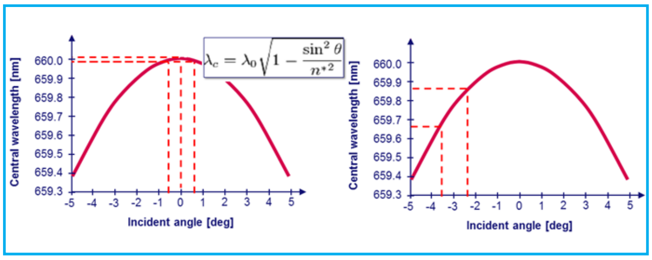

Figure 3 - Central wavelength as function of incident angle. The left plot shows that at direct incidence (0 deg.) the divergence (of +/-0.5 deg. in this case) causes little broadening around the maximum a central wavelength (660nm in this particular case). The right plot shows that increasing the incident angle, decreases the central wavelength. But it also shows that the divergence causes a range of wavelengths to be covered, resulting in a broadening of the band shape.

For the first question a model based on first principles was developed and compared to measurements performed by the spectrometer. A cartoon of the experimental setup is shown in Figure 4. The filter was mounted on a rotation stage, hence controlling the incident angle. The divergence was controlled by setting the aperture diameter. After the filter a lens coupled the light into an optical fibre that was connected to the spectrometer.

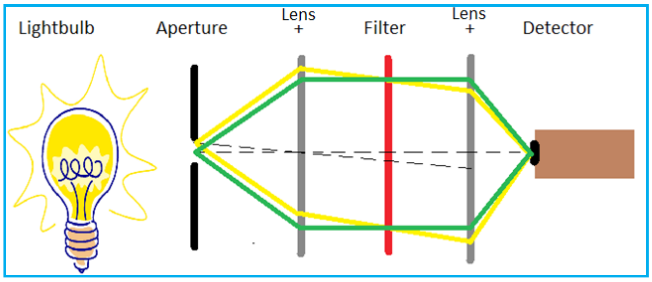

Figure 4 - Test setup for the filter band shape measurements for different divergences and different incident angles.

Figure 5 shows the measured filter band pass and the initial model, based on the relation given in Figure 3, for 2 incident angles (0 and 5 degrees) and a divergence of 1.1 degree. It is immediately clear that the initial model could be improved. Especially the predicted band shape width under large incident angles was significantly smaller than predicted by the initial model (which is in fact an advantage). In Figure 6 the central wavelength of the filter and its FWHM (full width half maximum) are plotted against the incident angle for 2 different divergence settings (0.86 deg. and 1.43 deg.). It shows that the model correctly predicted the shift in central wavelength, but that that width is over estimated. The overestimation of the width increased with incident angle and with divergence.

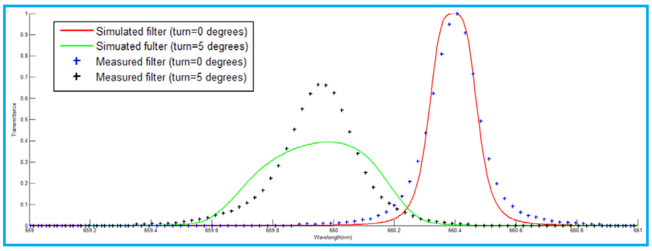

Figure 5 - Measured and modeled filter band shapes for 2 incident angles (0 and 5 degrees) and a divergence of 1.1 degree.

What is particularly of interest is the fact that the measured width seems to be independent (or only very weakly dependent) of the divergence. This was not expected,

Versatile spectrometry in an educational environment

M. de Bock, Science and Technology of Nuclear Fusion, Applied Physics,
Eindhoven University of Technology, The Netherlands (November 2012)

Application Note

because the relation given in Figure 3 clearly shows that the band of wavelengths transmitted increases with increasing divergence.

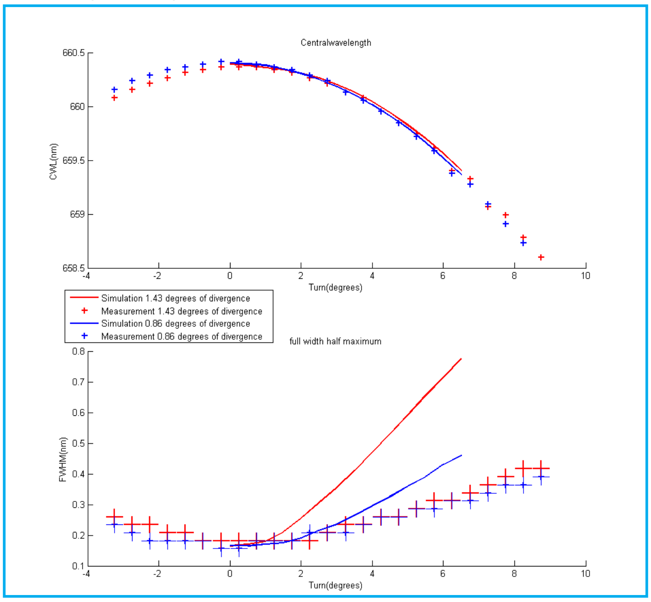

Figure 6 - Central wavelength and FWHM, measured and modelled, as a function of incident angle for 2 different divergence settings.

Two hypotheses were proposed to account for the difference between the model and the measurements:

1. The rays at larger angles could be reflected rather than transmitted.
2. Due to the finite diameter of the filter and lenses, the rays at larger angles are possible not collected by the fibre.

Implementing the Fresnel equations could quickly test the former. However, these showed that no significant effect is to be expected for incident angles smaller than 10 degrees, ruling out this hypothesis. The second hypothesis could not be checked within the scope of this bachelor project (due to time limitations) and is a subject for further study.

To be able to predict the band shape correctly, the fact that rays at large angles seemed to have less of an impact on the band shape was introduced in the model as a phenomenological weighting factor

$$W(\theta, \theta_{inc}, \delta\theta) = [\cos(0.6(\theta_{inc} - \theta))]^{12 \cdot \delta\theta}$$

where θ_{inc} is the incident angle (i.e. the angle under which the filter is turned, and hence the angle around which the rays are distributed), θ is the angle of the ray and $\delta\theta$ is the divergence. The exact form of the weighting factor was determined from measurements over a wide range of incident angles and divergences. However, as mentioned above, the physical meaning is as yet not clarified and subject of further study. With this weighting factor the model could be brought in agreement with the measurements, as shown in Figure 7.

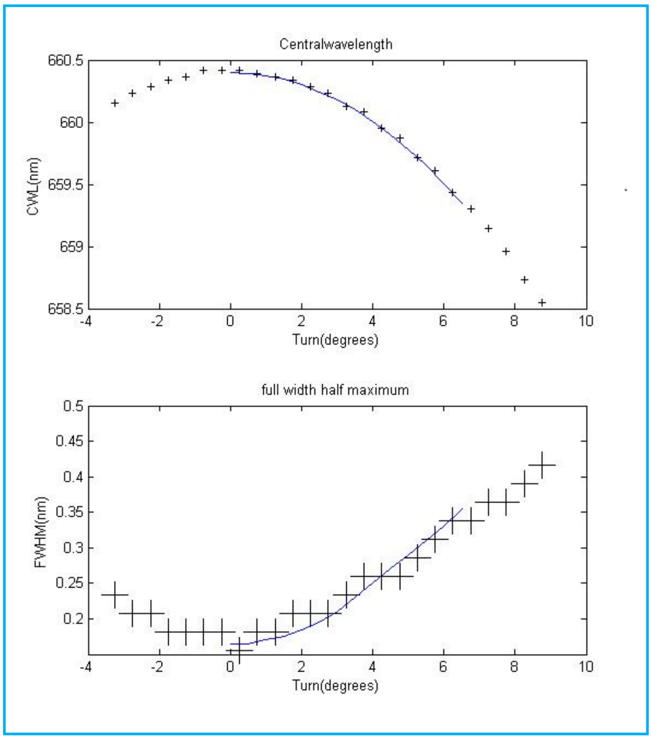

Figure 7 - Central wavelength and FWHM, measured and modelled including weighting factor, as a function of incident angle for a 1.1 degree divergence.

Velocity distribution of fast ions in a fusor

The second student project focused on a different type of fusion reactor: a Fusor. Fusor are the simplest type of fusion reactors: A negatively charged, spherical and transparent grid, placed in the centre of a spherical vacuum vessel at ground potential, accelerates ions towards that centre where they can collide with each other and undergo a fusion reaction (if the velocity is high enough, hence the negative potential large enough). The principle is shown in Figure 8.

M. de Bock, Science and Technology of Nuclear Fusion, Applied Physics,
Eindhoven University of Technology, The Netherlands (November 2012)

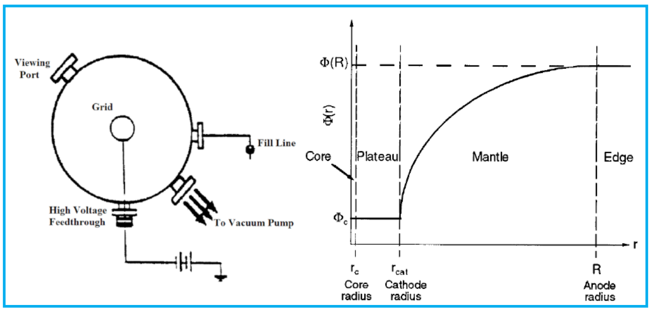

Figure 8 - The left plot shows a schematic picture of a fusor. The right plot shows the potential profile in vacuum.

Unfortunately, a fusor is not capable of producing net energy because most of the collisions are not between the accelerated fast ions themselves, but between such a fast ion and the electrons of the background gas/plasma. The latter then lose the energy they gain from the fast ions, both through bremsstrahlung and due to the fact electrons are not confined by the negative potential. Nonetheless, a fusor is a useful device either as neutron source or as a research device e.g. to study the interaction between fast ions and a background plasma, which is also of importance for more promising (but significantly more expensive) devices like the tokamak presented in the previous section. Therefore, a fusor was built at the TU/e, of which a picture is shown in Figure 9.

Figure 9 - The left picture shows the exterior of the fusor (before the voltage power supply and diagnostics were installed). The right picture shows the interior during operation.

In an ideal situation the ions originate at the edge of the fusor, are accelerated over the full (vacuum) potential shown in Figure 8 and hence all have the same velocity. In reality, however, ions originate throughout the device resulting in a velocity distribution. Moreover, the potential profile is not perfectly symmetric, due to the 'holes' in the grid, and will be modified by the presence of the ions itself. This in turn will affect the velocity distribution. The aim of the student project described here was to derive the velocity distribution from optical spectroscopy such that it could be compared used to infer properties of the potential profile.

For this project the fusor was operated with hydrogen gas. With a collection lens at one of the viewing ports the centre of the fusor was imaged onto an optical fibre that was coupled into the spectrometer which is centred around the Balmer-α wavelength of 656nm. The Balmer-α spectrum consists of 2 components:

1. The thermal emission
2. Fast (charge exchange) CX-emission

The former is emitted by the background H-atoms that are excited due to collisions with the fast ions. It has a Doppler broadening due to the thermal velocity distribution of the background gas/plasma. Because of the very low temperature of the background (a few eV), the thermal contribution is dominated by the instrument function of the spectrometer and manifests itself as a sharp peak (with the instrument width) in the centre of the spectrum (see Figure 10.

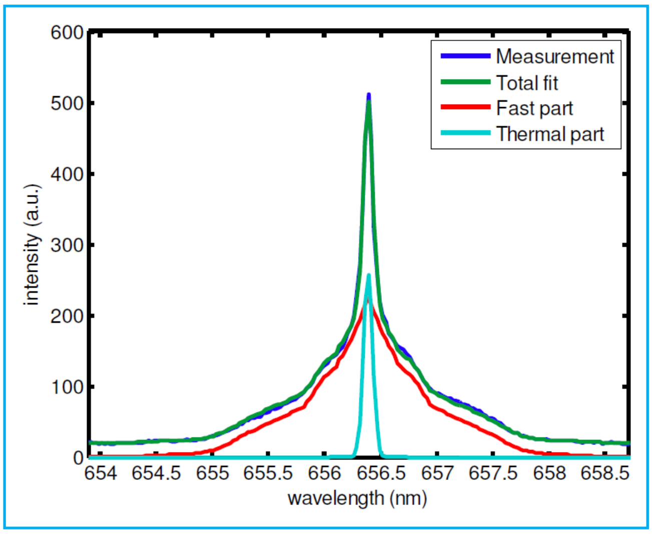

Figure 10 - Measured Balmer-α specttum with the fit and the contribution thermal and fast ion components of the fit.

The fast CX-emission is a result of the charge exchange reaction, whereby a background atom exchanges its electron with a fast ion:

$$H^{+}_{fast} + H_{background} \rightarrow H^{*}_{fast} + H^{+}_{background} \rightarrow H_{fast} + h\nu + H^{+}_{backgroud}$$

In the charge exchange reaction the velocity of the fast ion is preserved, resulting in a fast atom after the charge

M. de Bock, Science and Technology of Nuclear Fusion, Applied Physics,
Eindhoven University of Technology, The Netherlands (November 2012)

exchange reaction. This fast atom will be in an excited state and emit light when it cascades down to the ground state. The Doppler shift will depend on the velocity of the fast ion and hence the Doppler broadening of the CX-spectrum will depend on the velocity distribution of (all) fast ions. Because the (maximum) energy of the fast ions is given by the applied voltage in fusor, and because this voltage is typically of the order of a few tens of kV, the broadening of the fast CX part of the spectrum is significantly larger that the instrument function and is clearly seen as wings in Figure 10.

Assuming spherical symmetry the velocity distribution of the fast ions can be reconstructed from the fast CX-spectrum. This is shown in Figure 11. The first observation is that the velocity distribution is clearly not Gaussian and hence not thermal, as expected. Furthermore, a step in the distribution, indicated by ***c*** in Figure 11, is commonly observed at a velocity much lower than the maximum velocity corresponding to the applied voltage (5kV in the shown example which corresponds to 10^6 m/s). Finally, a peak the velocity distribution is seen at even lower velocities, indicated by ***b*** in Figure 11.

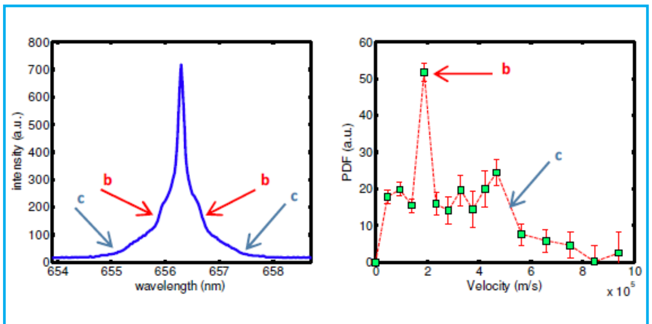

Figure 11 - Fast ion velocity distribution derived from the fast CX-spectrum for fusor operation at ~5kV.

The exact meaning of these features in the velocity distribution is still under investigation. Hypotheses have been proposed, including a lowering of the total potential due to the positively charged ions and trapped particles in potential wells present due to the "holes" in the grid. Further research is on-going to verify these hypotheses.

Conclusion

The Shamrock SR-500i-B1 / iVac DR324B-FI spectrometer system proved very useful in an educational environment thanks to the ease of use, its mobility and modular structure. It is used in many of our student projects, often in an "interleaved" manner (i.e. one day coupled to a test setup in one lab, moved to another lab the next day and moved back again etc.). As an example we have presented two student projects where the spectral measurements provided in new insights and triggered new questions for further research.

Contact

Dr. Maarten de Bock
Assistant Professor
Science and Technology of Nuclear Fusion
Department of Applied Physics
Eindhoven University of Technology
Den Dolech 2
5612 AZ Eindhoven
The Netherlands

Phone: +31 (40) 2472942
E-Mail: m.f.m.d.bock@tue.nl
Web: http://phys.tue.nl/fusion